Available online at www.sciencedirect.com
ScienceDirect
Applied Catalysis B: Environmental 79 (2008) 81–88
APPLIED CATALYSIS B: ENVIRONMENTAL
www.elsevier.com/locate/apcatb

Dinitrogen photofixation properties of different titanium oxides in conducting polymer/titanium oxide hybrid systems

K. Hoshino *, R. Kuchii, T. Ogawa

Faculty of Engineering, Chiba University, 1-33 Yayoi, Inage, Chiba 263-8522, Japan

Received 4 April 2007; received in revised form 2 October 2007; accepted 8 October 2007
Available online 13 October 2007

Abstract

Titanium oxide layers prepared by hard (rutile and anatase types) and soft processes (anodic amorphous oxides prepared in an aqueous phosphoric, TiO_x^w, and a dichloromethane/electrolyte solution, TiO_x^o) were brought into contact with the ClO_4^--doped poly(3-methylthiophene) (P3MeT) film, and their ability to photofix atmospheric dinitrogen was compared. The comparisons revealed that the latter junctions using amorphous oxides produced larger amount of N_2-fixation products than the former two junctions and that the P3MeT/TiO_x^w junction exhibited a higher N_2-fixation rate than the P3MeT/TiO_x^o cell. The TiO_x^w and TiO_x^o layers were characterized by transmission electron microscopic observations, X-ray electron dispersive analysis, and selected area electron diffraction measurements, and the higher activity of the TiO_x^w layer was rationalized on the basis of the contact potential difference measurements. Additionally, the dependences of the N_2-fixation yield on the photoirradiation time, P3MeT film thickness, and anodizing potential during the formation of the TiO_x^w were investigated using the most active P3MeT/TiO_x^w junction cell.

Keywords: Nitrogen fixation; Conducting polymers; Titanium oxide; Anodic titanium oxide; Light-to-chemical energy conversion

1. Introduction

Industrial ammonia synthesis by the Haber–Bosch process [1], in which hydrogen gas reacts with nitrogen gas to yield ammonia in the presence of catalysts under high pressure and temperature, is a well-established dinitrogen fixation process and, therefore, its feasibility to be replaced by other processes seems remote [2]. However, artificial dinitrogen fixation under milder conditions has been a chemical issue of great significance, since the reduction in the input energy during the fixation process and no use of dihydrogen from a natural gas may be preferred from the viewpoints of cost and environmental preservation. This significance has directed many chemists to find chemical [3,4], electrochemical [5,6], and photochemical routes [7,8] to fix dinitrogen under mild conditions. Finding these new routes is still continuing and some intriguing materials and systems for the N_2-fixation were quite recently proposed. Vettraino et al. prepared a reduced mesoporous titanium oxide on which the conversion of dinitrogen to ammonia occurred [9]. Rusina et al. demonstrated the photofixation of dinitrogen to ammonia and nitrate using an $Fe_2Ti_2O_7$ photocatalyst and the visible-light sensitivity of the reaction [10,11]. The electrochemical reduction of N_2 in molten salts was reported by Murakami et al. in which the electroreduction product, N_3^-, is coupled with H_2 at an anode to give NH_3 [12]. Nishibayashi et al. found that visible-light irradiation of an aqueous solution containing the C_{60}:γ-cyclodextrin (1:2) complex and $Na_2S_2O_4$ at 60 °C gave ammonia [13]. The plasma-induced fixing of dinitrogen during 1-butanol polymerization was reported by Matsuura et al. who suggested that this novel technique could be applied to fix gases into a liquid at the molecular level [14]. Köleli and Röpke found that the electroreduction of N_2 to ammonia occurred at a polyaniline electrode in a methanol/H_2SO_4 solution under an N_2-pressure of 50 bar [15].

Our group also reported a novel system for the photofixation of dinitrogen at ambient pressure and temperature [16,17]. The system consists of a layered structure of anodic titanium oxide (TiO_x) and a conducting polymer. Photoirradiation of this organic–inorganic p-n heterojunction induced the fixation of

* Corresponding author. Tel.: +81 43 290 3478; fax: +81 43 290 3490.
E-mail address: k_hoshino@faculty.chiba-u.jp (K. Hoshino).

0926-3373/$ – see front matter © 2007 Elsevier B.V. All rights reserved.
doi:10.1016/j.apcatb.2007.10.007

atmospheric dinitrogen into ammonia and an ammonium salt. The effects of the type and preparation conditions of the conducting polymers on the amount of the N_2-fixation products were investigated in some detail [18,19]; however, little information has been provided on the nature of the TiO_x and its ability to fix N_2 compared to the conventional titanium oxides [20] though the role of the TiO_x should be the key to our N_2-fixation process. In the present study, we prepared four types of titanium oxide films, and examined their activity towards the N_2-fixation. Additionally, the detailed N_2-fixation properties of the most active titanium oxide will be described.

2. Experimental

2.1. Preparation of titanium oxides and poly(3-methylthiophene) films

Four types of titanium oxide films were prepared by solution coating, sintering, and anodic oxidation methods. Anatase titanium oxide film was prepared by spin-coating (1000 rpm, 20 s) an aqueous dispersion of titanium oxide particles (photocatalytic hydrosol STS-21, Ishihara Sangyo Kaisha Ltd.) on an indium–tin-oxide-coated glass (ITO, Geomatech Co., 10 $\Omega\ sq^{-1}$). The concentration of the titanium oxide and the particle size in the dispersion are 40 wt% and 20 nm, respectively [21]. The obtained coating was dried at 80 °C for 15 min and then sintered at 400 °C for 30 min to give a 3.3 μm thick film.

The rutile titanium oxide layer was prepared by firing a titanium plate using a piezo gas burner (Yoshinaga Co., model GB2001, 800–1300 °C) for 4 min [22], followed by ultrasonic washing in trichloroethylene, acetone, and then ethanol to give a 0.85 μm thick film. The titanium plate (>99.5% purity, Sumitomo Metal Industries Ltd.) contains impurities such as Fe (0.250%), K (0.013%), O (0.200%), and N (0.0050%).

The anodic oxide films prepared in a CH_2Cl_2 solution, TiO_x^o, have been exclusively employed in our N_2-fixation experiments and their preparation has already been described elsewhere, but will be briefly outlined here [16,18]. The titanium plate was anodized in a CH_2Cl_2 (Kanto Chemical Co. Ltd., spectroscopic grade, >99.5%) solution containing 0.1 M tetrabutylammonium perchlorate (TBAP, Tokyo Kasei Kogyo Co. Ltd., >98%) at 20 °C using a two-electrode-type cell. The counter electrode was a Pt plate. The potential applied to the titanium plate was 5 V with respect to the Pt plate. The area of the two electrodes exposed to the electrolyte solution was 2.0 cm^2, delimited by O-rings. Prior to the anodic oxidation, the titanium plate was degreased and etched by dipping in aqueous HF (5%, 5 min) and then in an HF (1%)/HNO_3 (3%)/H_2O_2 (10%) mixture for 30 s followed by washing in water for 1 min. Additionally, the anodic oxide films were also formed in a phosphoric acid solution (0.85 wt%, Kanto Chemical Co. Ltd.) at 20 °C. The typical potential applied to the titanium plate was 10 V versus the counter Pt plate at which a brownish yellow oxide layer, TiO_x^w, was formed on the titanium plate. These TiO_x layers were ultrasonically washed in trichloroethylene, acetone, and ethanol (10 min each).

Poly(3-methylthiophene) (abbreviated as P3MeT) films were potentiostatically deposited on the titanium oxide layers at 70 V versus the counter Pt plate and 13 °C using a dichloromethane solution containing 3-methylthiophene (0.1 M) and TBAP (0.1 M) in the two-electrode-type cell. The typical amount of electricity (Q) for the electropolymerization was 250 mC cm^{-2} at which the P3MeT film of 0.92 ± 0.06 μm thickness was formed. Prior to the electropolymerization, 3-methylthiophene was purified by distillation.

2.2. N_2-fixation procedures and determination of fixation products

Illumination of the P3MeT/titanium oxides samples by white light from a pseudosolar lamp (Xenon lamp, Seric Ltd., 100 W) equipped with an IR-cut filter (BFIRC) was performed through a quartz window having a 220 mm diameter attached to an acrylic container (500 mm × 500 mm × 750 mm) which contains the samples, digital thermo-hygrometer, aqueous electrolyte solution, and air. The pseudosolar lamp produces reduced output in the wavelength region above 700 nm compared to the sun light (AM 1.5) and exhibits negligible irradiance above 780 nm due to the action of the IR-cut filter, and therefore, the irradiance is in the wavelength range of 300–780 nm (see supplementary material). In our previous study, we demonstrated the visible-light activity of the P3MeT/TiO_x^o junction cell. Based on this demonstration, we used the light source with visible-light irradiance in this study. The relative humidity inside the container was controlled using the aqueous electrolyte (KCl) solution [23] in a laboratory dish, which was then placed in the acrylic container; the container was placed in an air-conditioned room, thus keeping the atmosphere in it at approximately 24 °C and 40% RH throughout the illumination. The light intensity was measured by a Model MS-601 pyranometer (EKO Co.).

The amount of N_2-fixation products per unit area of the P3MeT/titanium oxides samples, η, was determined by the following indo-naphthol method [24] which can be used for the quantification of NH_3 and NH_4^+. After illumination of the samples, they were immersed in 6 ml of distilled-deionized water and stored for 2 min during which the fixation products were dissolved in water. To 5 ml of the above aqueous solution, 1 ml of an NaClO aqueous solution (concentration of active chlorine = 0.10 wt%, Kanto Chemical Co. Ltd.) was added, followed by shaking, standing for 1 min, adding an aqueous NaOH (0.20 M, 3 ml), and shaking. To the resulting solution, 1.5 ml of a 5.0 wt% acetone solution of 1-naphthol (Kanto Chemical Co. Ltd., 99.0%) was added. The solution was diluted with water until the total volume of the solution was 25 ml. After standing for 5 min, the visible absorption spectrum of the obtained solution was recorded which showed a well-defined absorption maximum at 720 nm (the light-path length of a quartz cell was 5 cm). The molar absorption coefficient of the peak was determined to be $1.68 \times 10^3\ M^{-1}\ cm^{-1}$ from the working curve for the $NH_4^+ClO_4^-$ aqueous solutions.

2.3. Characterization

The cross-sections of TiO_x were observed by transmission electron microscopy (TEM, accelerating voltage = 200 kV) using a Hitachi FE-TEM HF2200 equipped with an energy-dispersive X-ray spectrometer (EDS, Noran Vantage EDS system). Selected area electron diffraction (SAED) was employed to study the structures of the TiO_x. The determination of the P3MeT film thickness and the observation of the film surface after the white light irradiation were carried out using a Topcon ABT-32 scanning electron microscope operating at an accelerating voltage of 15 kV. The chemical activity of the TiO_x was investigated by measuring the contact potential difference (CPD) with respect to an Au reference film [22]. A Trek 320B electrostatic voltmeter [25] was used to measure the CPD values on a 10 V scale with a precision of ±0.01 V.

3. Results and discussion

3.1. N_2-fixation activity of four types of titanium oxide layers

Four types of titanium oxides were compared with respect to the N_2-fixation activity. However, no structural feature of the TiO_x layers has been reported, and accordingly, their structural characterization was carried out by TEM observations coupled with electron diffraction measurements and EDS measurements before the comparison. Fig. 1 shows the TEM images of the cross-sections of the TiO_x^o (a) and TiO_x^w layers (b). The former and the latter thicknesses were 6 and 30 nm, respectively. Though not shown here, the EDS spectra of these layers revealed the presence of Ti and O, confirming that they are titanium oxide compounds. No lattice fringe was observed in the cross-sectional images, being in contrast to the crystalline texture of the underlying titanium metal and suggesting the amorphous structure of the TiO_x layers. This suggestion was confirmed by the SAED measurements. The insets in parts (a) and (b) show the SAED patterns of the TiO_x^o and TiO_x^w layers, respectively. The haloes in the patterns indicate that the TiO_x layers are amorphous in structure. The diffraction spots other than the halo seen in part b can be indexed as the base titanium metal (ICDD diffraction file: 44-1294); hence, we can conclude that the TiO_x^w layer only shows the halo pattern. The amorphous nature of the TiO_x layers agrees well with the postulated structure of the anodic titanium oxides prepared at voltages up to ca. 20 V [26]. The electron beam employed in the SAED measurements has a diameter of several tens of nanometers, so that the diffraction spots from the base titanium metal were seen in the TiO_x^w layer (30 nm thick). On the other hand, the SAED patterns of the thinner TiO_x^o layer (6 nm thick) was obtained from a specific region in which the TiO_x^o layer was partially peeled off from the titanium metal in order to avoid the diffraction from the titanium metal.

Table 1
Results of N_2-fixation experiments using various titanium oxide layers[a]

Titanium oxide	η (mmol m^{-2})[a]
Rutile type	1.1
Anatase type	1.5
Amorphous type, TiO_x^o	2.1
Amorphous type, TiO_x^w	2.5

[a] Photoirradiation conditions: white light intensity, 260 W m^{-2}; irradiation time, 7 days; temperature, 24 °C; relative humidity, ca. 40% RH.

The P3MeT film was deposited on the four titanium oxide layers and the photofixation experiments were carried out. The P3MeT film (thickness = 0.92 ± 0.06 μm) was prepared under the typical conditions described in the experimental section. The resultant P3MeT/titanium oxide junctions were exposed to the white light (260 W m^{-2}, 7 days) after being washed in dichloromethane and dried at room temperature in the dark. Table 1 shows the results of the N_2-fixation experiments using various titanium oxide layers. The N_2-fixation reaction occurred in all the types of titanium oxide, however, the value of η was dependent on the type. The two P3MeT/TiO_x junctions fix more nitrogen than the other two junction samples using the rutile and anatase titanium oxides, and the P3MeT/TiO_x^w gave the highest result. The understanding of the difference in the N_2-fixation activity may require the mechanism involving the reaction scheme and the sites in the junction sample at which the electron transfer and the subsequent steps occur. At the present stage of our research, little is known about the mechanism, but such mechanistic studies are now under way which involve the surface properties of the TiO_x, the distribution of the N_2-fixation products along the P3MeT film thickness, the role of the P3MeT film in the reaction, etc., the details of which will be reported elsewhere.

About three decades ago, the synthesis of ammonia over photoirradiated titanium oxide powders doped with iron was reported by Schrauzer and Guth in which the photosplitting of water is coupled with the chemisorption of dinitrogen at

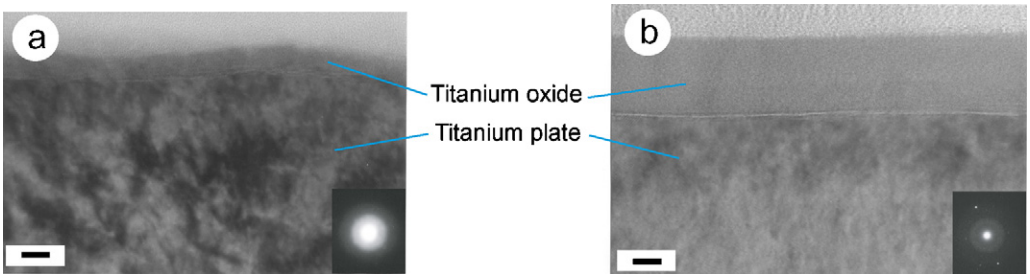

Fig. 1. Cross-sectional TEM images of the TiO_x^o (a) and TiO_x^w layers (b) on a titanium metal plate. Insets show the SAED patterns of the respective oxide layers. Scale bars: 10 nm.

oxygen-deficient sites (or Ti^{3+} sites abbreviated as $Ti^{3+}\square$) to produce ammonia [7,27]. The key to successful N_2-fixation is the presence of the $Ti^{3+}\square$ sites which adsorb water (to yield hydrogen for the reduction of N_2) and nitrogen (to yield ammonia) [28]. If our N_2-fixation is based on the Schrauzer's process, it would consist of ammonia formation at the junction interface and the partial conversion of ammonia into an ammonium salt in the bulk of the P3MeT film. This assumption predicts that the $Ti^{3+}\square$ sites also play crucial role in our fixation system. If we make the further assumption that fewer oxygen deficiencies are formed on the rutile and anatase titanium oxides prepared by hard (energy-consuming) processes than on the TiO_x layers prepared by soft processes, the difference in the η value in Table 1 may be accounted for.

Fig. 2 shows SEM images of the P3MeT surfaces obtained after the photoirradiation (260 W cm^{-2}, 7 days) of the rutile oxide/P3MeT (a), anatase oxide/P3MeT (b), TiO^o_x/P3MeT (c), and TiO^w_x/P3MeT junctions (d). The bright cylindrical needles in images (a), (c), and (d) are assigned to ammonium perchlorate crystals [16,17]. On the other hand, the shape of the crystals on the anatase oxide/P3MeT (image (b)) is conglomerate. Previously, we reported that the crystal shape was dependent on the kind of conducting polymer in contact with the TiO^o_x and that needles were formed using polythiophene, polybithiophene, and polyvinylcarbazole, while the conglomerates were produced using polypyrrole [18]. A specific feature common between the polypyrrole film on the TiO^o_x and the P3MeT film on the anatase titanium oxide is the smooth structure of the film, being in contrast to the ragged structure of the other films. These observations indicate that the crystal growth of $NH_4^+ClO_4^-$ in a cylindrical fashion requires a small space in the conducting polymer film bulk. The nucleation of $NH_4^+ClO_4^-$ would probably occur throughout the P3MeT bulk. In the ragged film, nuclear growth might partly occur in a cylindrical fashion through the small spaces among the polymer granules and the cylinders extend their length at the roots. On the other hand, the nucleus might increase its number in the smooth films during the fixation reaction, since it cannot grow in the cylindrical form due to the lack of space in the polymer film.

3.2. N_2-fixation rates of the P3MeT/TiO_x junctions

In most of the N_2-fixation processes using the Schrauzer's method, the production rate of NH_3 significantly declines after a few to several tens of hours. This decline was explained by the deactivation of TiO_2 and/or the delayed photooxidation of NH_3 to NO_x [28,29]. On the other hand, no decline was observed in our fixation system using the P3MeT/TiO^o_x system [18]. In this section, the initial fixation rate and the final fixation yield of the P3MeT/TiO^w_x junction, the most active junction, were investigated and compared with those of the P3MeT/TiO^o_x.

Fig. 3 shows the dependence of η on the irradiation time, t, of the white light (260 W m^{-2}) for the P3MeT/TiO^w_x (closed circles) and the P3MeT/TiO^o_x junctions (open circles). The data on the latter junction has already been reported [18], however, we reinvestigated the dependence since the light source and intensity employed in the report were different from the present case. In both of the junctions, η linearly increases with t at first, but then tapers off after t reaches ca. 2 weeks. The initial fixation rates of 17 and 14 μmol of fixation products per 1 m^2-TiO_x and 1 h were obtained for the P3MeT/TiO^w_x and P3MeT/

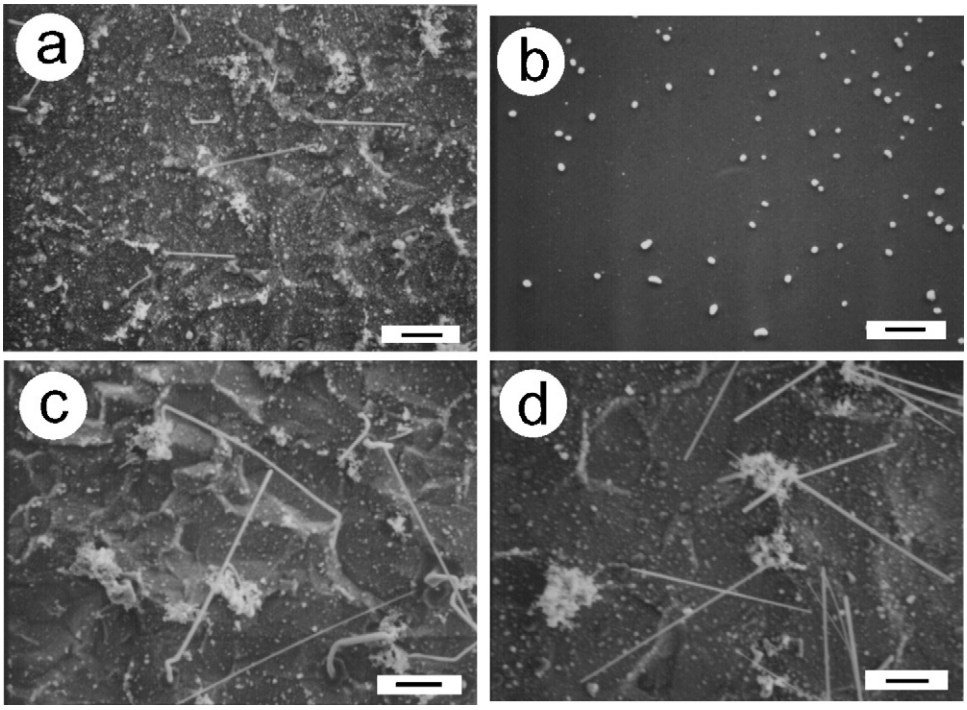

Fig. 2. SEM images of the P3MeT surfaces in contact with the rutile titanium oxide (a), anatase oxide (b), amorphous TiO^o_x layer (c), and amorphous TiO^w_x (d) layer after the white light irradiation (260 W m^{-2}) for 7 days. Scale bars: (a), 20 μm; (b), 10 μm; (c), 20 μm; (d), 20 μm.

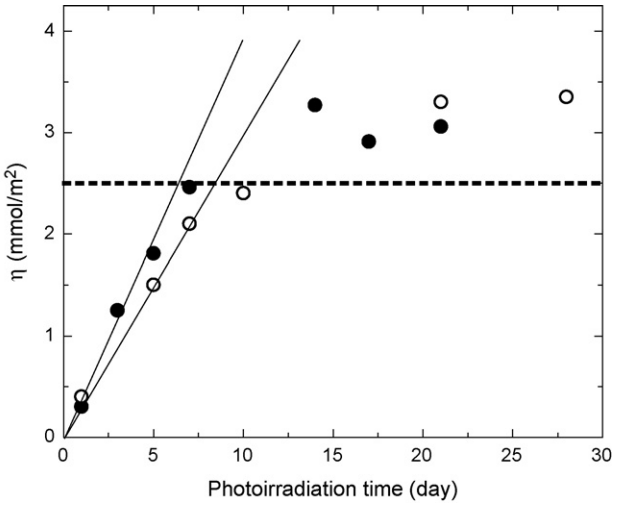

Fig. 3. Photoirradiation time (t) dependence of the amount of N_2-fixation products, η, for the P3MeT/TiO_x^w (●) and the P3MeT/TiO_x^o (○) junction cells. White light intensity: 260 W m^{-2}. The dotted line indicates the concentration of ClO_4^- ion doped in the P3MeT film.

TiO_x^o junctions, respectively. This result indicates the higher N_2-fixation activity of the TiO_x^w compared to the TiO_x^o. If the activity is based on the density of the oxygen deficiency ($Ti^{3+}\square$) in the TiO_x as described in Section 3.1, the results suggest that the TiO_x^w has more oxygen deficiencies than the TiO_x^o. Rothschild et al. measured the CPD's of the reduced and oxidized titanium oxide films with respect to an Au probe, and showed that the dark CPD of the former film is more positive than the latter [30]. They explained the difference in terms of the chemisorption of water molecules on the reduced (or oxygen deficient) oxide surface. This demonstrates that the CPD value is a good indication of the relative abundance of the oxygen deficiency, and therefore, the CPD measurements were carried out with the TiO_x^w and TiO_x^o samples. The CPD values of +0.34 and +0.31 V versus Au were obtained for the TiO_x^w and TiO_x^o samples, respectively, thus supporting the higher N_2-fixation activity of the P3MeT/TiO_x^w junction compared to the P3MeT/TiO_x^o. Our previous study [18] on the X-ray photoelectron spectroscopic analyses of the P3MeT bulk revealed that $NH_4^+ClO_4^-$ and NH_3 were produced as the fixation products and accumulated in the P3MeT film. The amount of $NH_4^+ClO_4^-$ is dependent on the amount of ClO_4^- ions doped in the P3MeT film that was determined to be 2.5 mmol m^{-2} by the EDS analysis. Thus the saturation values of η, i.e., final yields for the two junctions ($\eta = 3.2$ mmol m^{-2}) imply that $NH_4^+ClO_4^-$ and NH_3 were produced in the mol ratio of 78:22.

One of the specific features of our fixation reaction is to obtain the solid compound, $NH_4^+ClO_4^-$ cylinders, as the major product. Hence, we can view the progress of the reaction under the electron microscope. Fig. 4 shows the SEM images of the $NH_4^+ClO_4^-$ cylinders generated on the P3MeT/TiO_x^w junction by white light irradiation for 1 day (a), 3 days (b), 7 days (c), and 14 days (d). Increases in the size and abundance of the cylinders with t are clearly demonstrated in the images, confirming the monotonous increase in η with t in Fig. 3.

3.3. Effect of P3MeT film thickness

If we assume again that our N_2-fixation is initiated by ammonia formation at the junction interface, the thickness of

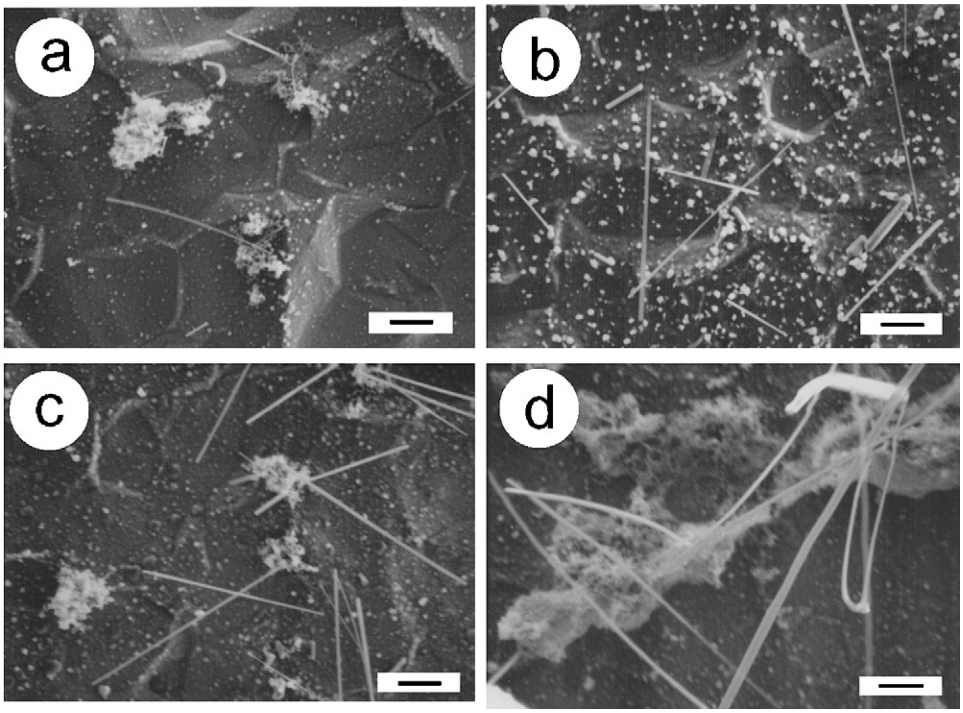

Fig. 4. Growth of N_2-fixation product, the $NH_4^+ClO_4^-$ crystals, on the P3MeT surfaces vs. the photoirradiation time, t: (a), t = 1 day; (b), t = 3 days; (c), t = 7 days; (d), t = 14 days. White light intensity: 260 W m^{-2}. Scale bars: 20 μm.

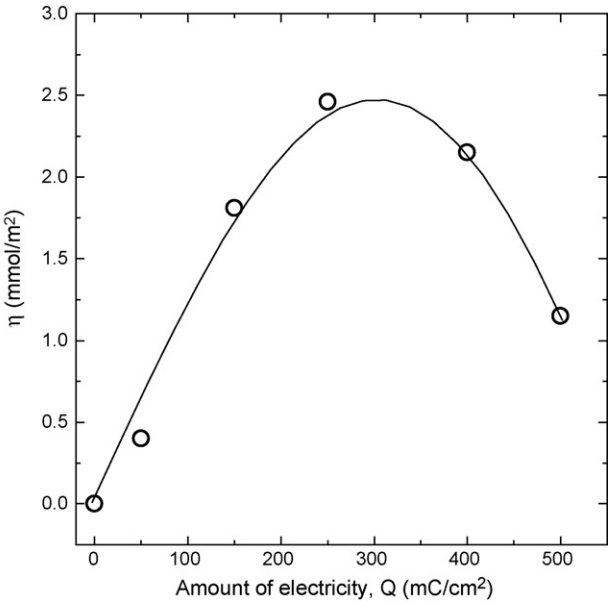

Fig. 5. Dependence of η on the amount of electricity passed during the electropolymerization of P3MeT at 13 °C, Q. The TiO_x layer was prepared at 10 V and 20 °C. The thickness of the P3MeT layer above ca. 1 μm cannot be defined due to the porous structure of the film. All of the samples were exposed to 260 W m^{-2} white light for 7 days.

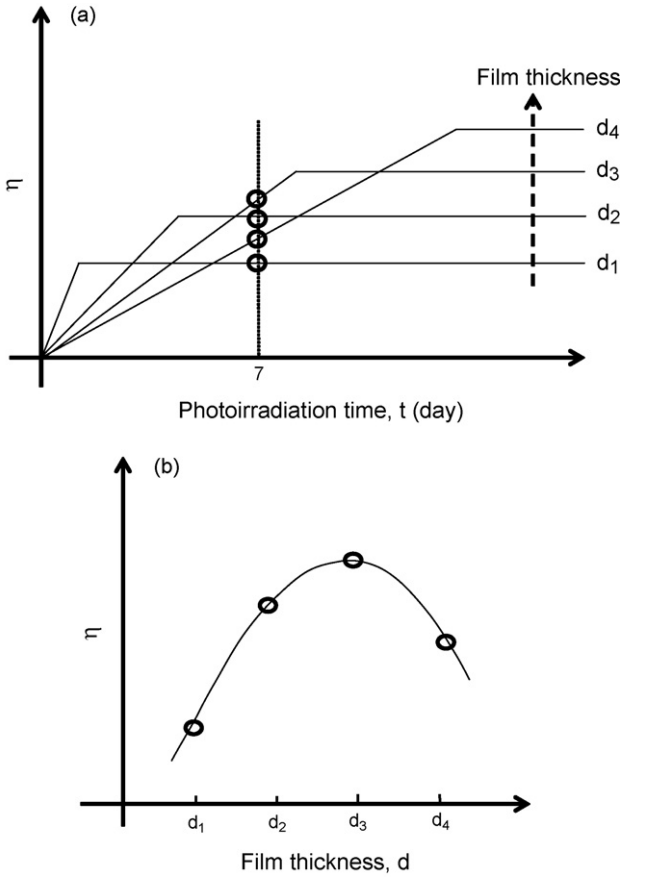

Fig. 6. Expected dependences of η on the photoirradiation time, t, (a) and the P3MeT film thickness, d, (b). The values of d increases in the order of $d_1 < d_2 < d_3 < d_4$.

the P3MeT film (d) may be one of the key parameters to determine η because of the panchromatic character of the film. Thus the relationship between η and d was investigated as shown in Fig. 5. The TiO_x^w layer and P3MeT film were prepared at 10 and 70 V, respectively, and all of the samples were exposed to 260 W m^{-2} white light for 7 days. The P3MeT layer compactly grew to d = ca. 1 μm, but any further deposition formed a rough and porous layer, and the value of d at Q = 50 mC cm^{-2} was difficult to measure due to the difficulty in separating the film from the TiO_x^w; hence, the value of Q was plotted as the abscissa instead of the thickness. However, a rough estimate of d can be made using the following empirical formula: d (μm) = 3.2 × 10^{-3} Q (mC cm^{-2}).

Fig. 3 consists of a region in which a constant fixation rate is maintained and a plateau region. Considering that an increase in d causes a reduction in the number of photons reaching the junction interface and an increase in the concentration of ClO_4^- available for the N_2-fixation reaction, it may well be that the increase in d causes a decrease in the slope of the former region (i.e., initial fixation rate) and an increase in the plateau value of the latter region. This is schematically illustrated in part (a) of Fig. 6 in which the expected η–t curves are plotted as a function of d ($d_1 < d_2 < d_3 < d_4$). Under the condition of a constant illumination time (7 days in the present case), η would be saturated before the end of the 7 day illumination and thus limited by the plateau value for the lower thicknesses (d_1 and d_2), while η would not reach saturation for the larger thicknesses (d_3 and d_4), and accordingly, would be determined by the initial fixation rate. Thus the dependence of η on d is qualitatively illustrated in part b of Fig. 6. The shape of the curve in Fig. 5 may be explained on the basis of these considerations which also predict that the value of d showing a maximum increase with the increasing illumination time and intensity.

3.4. Effect of anodizing potential

Another key factor affecting η would be the anodizing potential (E) at which the anodic titanium oxide is formed. In our previous study, the dependence of η on E was investigated for the P3MeT/TiO_x^o junction system, and it was found that the higher η values were obtained in the lower potential range ($E \leq$ ca. 10 V) and that the values of η decreased with the increasing E above E = ca. 10 V. However, no clear account was made of the dependence. Here we checked the dependence again using the P3MeT/TiO_x^w junction system and explained it in terms of the potential-dependent nature of the TiO_x^w layer.

Fig. 7 shows the dependence of η on E for the P3MeT/TiO_x^w junction system. The P3MeT layers were prepared at 70 V below E = 10 V and at 120 V above E = 30 V, since no homogeneous film was formed at 70 V under the condition of E = 30 V. The amount of electricity for the electropolymerization was 400 mC cm^{-2}. The average thickness of the P3MeT film was 1.4 ± 0.1 μm except for the case of E = 5 V where the

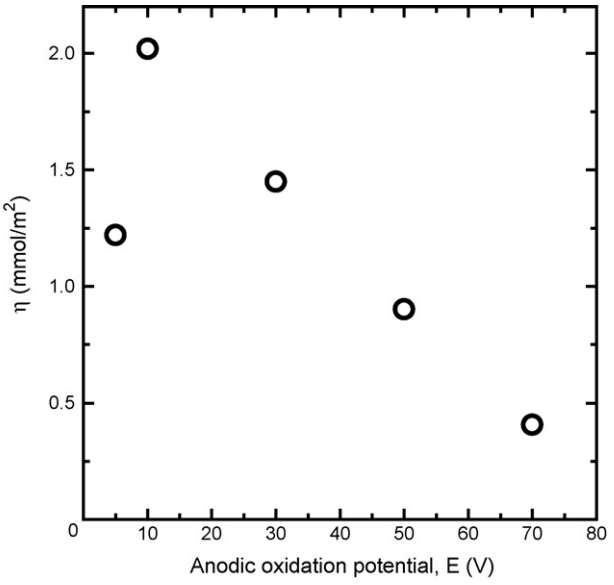

Fig. 7. Dependence of η on the anodic oxidation potential for the preparation of TiO_x^w at 20 °C, E. The P3MeT layers were prepared at 70 V ($E \leq 10$ V) and 120 V ($E \geq 30$ V) by passing 400 mC cm^{-2} of electricity. All of the samples were exposed to 260 W m^{-2} white light for 7 days.

thickness was too thin to be peeled off from the TiO_x^w layer and measured by the SEM observations. The smaller η value at $E = 5$ V may come from the smaller amount of available ClO_4^- anions due to the smaller thickness of the P3MeT film. The η value monotonously decreased with an increase in E above $E = 10$ V. Previously, we measured the current–voltage and capacitance–voltage characteristics of the P3MeT/TiO_x^o junctions prepared at $E = 5$ V and 20 V, and revealed that the chemical activity of the TiO_x^o surface of the former junction was much higher than that of the latter junction [31]. The result was reasonably explained by assuming that the oxygen-deficient site ($Ti^{3+}\square$) in the former TiO_x^o is more abundant than that in the latter. Armstrong et al. [32,33] and Shibata and Zhu [34] carried out the X-ray photoelectron spectroscopic measurements of anodic titanium oxide films and found that the Ti^{3+} species is involved in the oxide films. Pankuch et al. obtained the surface-enhanced Raman spectra of anodic titanium oxides, showing that the films formed at low potentials involve the Ti^{3+} species, but the films formed at high potentials do not [26]. In addition, the CPD values of the TiO_x^w layers prepared at 10 and 70 V were measured to be +0.34 and −0.19 V, respectively. As described in Section 3.2, the more positive value of the former TiO_x^w layer is an indication that it involves more abundant $Ti^{3+}\square$ sites than the latter. On the basis of these previously reported results and the CPD values measured in this study, the monotonous decrease in η with E in Fig. 6 is supposedly due to the decrease in the number of $Ti^{3+}\square$ sites with E.

4. Conclusions

We investigated the N_2-fixation activities of titanium oxide/P3MeT junctions in which the oxide layers were prepared by firing with a gas burner (rutile type), annealing of a solution-coated film (anatase), anodizing in an organic solution (amorphous), and anodizing in water (amorphous). We found that the highest activity was exhibited by the junction based on anodic titanium oxide prepared in water. This result can be explained by considering the density of the oxygen-deficient sites in the titanium oxide at which the adsorption, activation, and reduction of dinitrogen might occur. The effects of the photoirradiation time (t), P3MeT film thickness (d), and anodizing potential (E) on the amount of the N_2-fixation products were investigated using the most active junction of P3MeT and titanium oxide anodically prepared in water. The white light irradiation (260 W m^{-2}) of the most active junction produced the maximum yield of 3.2 mmol m^{-2} (for the production of NH_3 and NH_4ClO_4) under the conditions of d = ca. 0.9 μm, $E = 10$ V, and $t >$ ca. 14 days.

Acknowledgments

This work was partially supported by grants from NANOHANA COMPETITION 2006 for Fundamental and Applied Research in Natural Science and Engineering (The Futaba Electronics Memorial Foundation) to K.H. (No. 06B21).

Appendix A. Supplementary data

Supplementary data associated with this article can be found, in the online version, at doi:10.1016/j.apcatb.2007.10.007.

References

[1] F. Haber, Chem. Ztg. 34 (1910) 345.
[2] V. Smil, Sci. Am. (1997) 58.
[3] M.E. Vol'pin, V.B. Shur, E.G. Berkovich, Inorg. Chim. Acta 280 (1998) 264.
[4] G.J. Leigh, Science 279 (1998) 506.
[5] E.E. van Tamelen, B. Akermark, J. Am. Chem. Soc. 90 (1968) 4492.
[6] C.R. Dickson, A.J. Nozik, J. Am. Chem. Soc. 100 (1978) 8007.
[7] G.N. Schrauzer, T.D. Guth, J. Am. Chem. Soc. 99 (1977) 7189.
[8] K.T. Ranjit, B. Viswanathan, Indian J. Chem., Sect. A 35 (1996) 443.
[9] M. Vettraino, M. Trudeau, A.Y.H. Lo, R.W. Schurko, D. Antonelli, J. Am. Chem. Soc. 124 (2002) 9567.
[10] O. Rusina, O. Linnik, A. Eremenko, H. Kisch, Chem. Eur. J. 9 (2003) 561.
[11] O. Rusina, A. Eremenko, G. Frank, H.-P. Strunk, H. Kisch, Angew. Chem. Int. Ed. 40 (2001) 3993.
[12] T. Murakami, T. Nishikiori, T. Nohira, Y. Ito, J. Am. Chem. Soc. 125 (2003) 334.
[13] Y. Nishibayashi, M. Saito, S. Uemura, S. Takekuma, H. Takekuma, Z. Yoshida, Nature 428 (2004) 279.
[14] H. Matsuura, T. Tanikawa, H. Takaba, Y. Fujiwara, J. Phys. Chem. B 108 (2004) 17748.
[15] F. Köleli, T. Röpke, Appl. Catal. B: Environ. 62 (2006) 306.
[16] K. Hoshino, M. Inui, T. Kitamura, H. Kokado, Angew. Chem. Int. Ed. Engl. 39 (2000) 2509.
[17] K. Hoshino, Chem. Eur. J. 7 (2001) 2727.
[18] T. Ogawa, T. Kitamura, T. Shibuya, K. Hoshino, Electrochem. Commun. 6 (2004) 55.
[19] T. Ogawa, T. Igarashi, T. Kawanishi, T. Kitamura, K. Hoshino, J. Photopolym. Sci. Technol. 17 (2004) 143.
[20] K. Hoshino, T. Kitamura, Chem. Lett. (2000) 1120.
[21] http://www.iskweb.co.jp/functional_e/ISKWEB1-3-photocattop.htm.

[22] K. Hoshino, M. Inui, T. Kitamura, H. Kokado, Electrochem. Solid State Lett. 3 (2000) 426.
[23] T.D. Hong, S. Edgington, R.H. Ellis, M.A. de Muro, D. Moore, J. Invertebr. Pathol. 89 (2005) 136.
[24] M. Morita, K. Kogure, Nippon Kagaku Zasshi 84 (1963) 816.
[25] R.P.N. Veregin, D. Powell, C.P. Tripp, M.N.V. McDougall, M. Mahon, J. Imaging Sci. Technol. 36 (1997) 192.
[26] M. Pankuch, R. Bell, C.A. Melendres, Electrochim. Acta 38 (1993) 2777.
[27] G.N. Schrauzer, N. Strampach, L.N. Hui, M.R. Palmer, J. Salehi, Proc. Natl. Acad. Sci. U.S.A. 80 (1983) 3873.
[28] N.N. Rao, S. Dube, Mańjubala, P. Natarajan, Appl. Catal. B: Environ. 5 (1994) 33.
[29] O.A. Ileperuma, F.N.S. Weerasinghe, T.S.L. Bandara, Sol. Energy Mater. 19 (1989) 409.
[30] A. Rothschild, A. Levakov, Y. Shapira, N. Ashkenasy, Y. Komem, Surf. Sci. 532–535 (2003) 456.
[31] T. Ogawa, S. Takase, T. Kitamura, K. Hoshino, Hyomen Kagaku 25 (2004) 392.
[32] N.R. Armstrong, R.K. Quinn, Surf. Sci. 67 (1977) 451.
[33] C.N. Sayers, N.R. Armstrong, Surf. Sci. 77 (1978) 301.
[34] T. Shibata, Y.-C. Zhu, Denki Kagaku 61 (1993) 853.